

See discussions, stats, and author profiles for this publication at: <https://www.researchgate.net/publication/7343302>

Impedance Spectroscopy of OmpF Porin Reconstituted into a Mercury-Supported Lipid Bilayer

ARTICLE *in* LANGMUIR · FEBRUARY 2006

Impact Factor: 4.46 · DOI: 10.1021/la0520839 · Source: PubMed

CITATIONS

41

READS

11

3 AUTHORS:



Lucia Becucci

University of Florence

72 PUBLICATIONS 1,366 CITATIONS

SEE PROFILE



Maria Rosa Moncelli

University of Florence

121 PUBLICATIONS 2,028 CITATIONS

SEE PROFILE



Rolando Guidelli

University of Florence

226 PUBLICATIONS 3,782 CITATIONS

SEE PROFILE

Impedance Spectroscopy of OmpF Porin Reconstituted into a Mercury-Supported Lipid Bilayer

Lucia Becucci, Maria Rosa Moncelli, and Rolando Guidelli*

Department of Chemistry, Florence University, Via della Lastruccia 3,
50019 Sesto Fiorentino (Firenze), Italy

Received July 29, 2005. In Final Form: November 23, 2005

The channel-forming protein OmpF porin was incorporated in a biomimetic membrane consisting of a lipid bilayer tethered to a mercury electrode via a thiolipid, and it was investigated in aqueous KCl by electrochemical impedance spectroscopy. The impedance spectra, recorded from 1×10^{-2} to 1×10^5 Hz over a potential range of 0.7 V, were fitted to an equivalent circuit consisting of four RC meshes. The dependence of the resulting circuit elements upon the applied potential was interpreted on the basis of a general approximate approach based on a model of the electrified interphase and on the kinetics of the translocation of potassium and chloride ions across the lipid bilayer, assisted by the OmpF porin.

Introduction

Lipid bilayers tethered to a metal surface via a hydrophilic “spacer” may provide a friendly environment to channel-forming peptides and proteins, thus maintaining their functionally active state and allowing an investigation of their function. These tethered bilayer lipid membranes (tBLMs) also have potential for biosensor applications. The interposition of a hydrophilic layer between the metal surface and the lipid bilayer is of utmost importance to create the hydrophilic environment needed for the proper folding of the extramembrane section of integral proteins and to allow an ionic flow across the lipid bilayer, upon incorporation of an ion channel.¹ tBLMs are obtained by first self-assembling on a gold² or mercury³ electrode a monolayer of a thiolipid, which consists of a lipid tail and of a hydrophilic spacer terminated with a sulfhydryl or disulfide group for anchoring to the metal surface. A lipid monolayer is then self-assembled on top of the thiolipid monolayer by exploiting the hydrophobic interactions that bring the alkyl chains of the two monolayers in contact with each other, with the polar heads of the lipid turned toward the aqueous solution.

Thanks to its liquid nature, mercury provides a defect-free surface to the self-assembling film, and imparts a high fluidity to the tBLM by allowing the lateral movement of the thiolipid molecules anchored to its surface. On the other hand, tBLMs supported by mercury are not easily amenable to investigations

by surface-sensitive techniques, as opposed to tBLMs supported by gold.

In a recent work carried out in the present laboratory,⁴ use was made of a mercury-supported tBLM prepared with a particularly convenient thiolipid synthesized in the Max Planck Institute of Polymer Science, Mainz, and used by Naumann et al.⁵ for the preparation and characterization of tBLMs on gold. This thiolipid, named DPTL, consists of a tetraethyleneoxy (TEO) chain covalently linked to a lipoic acid residue for anchoring to the metal at one end, and bound via ether linkages to two phytanyl chains at the other end, as shown in Figure 1. The electrochemical impedance spectra recorded with this tBLM in aqueous 0.1 M KCl, upon incorporation of the ionophore valinomycin, were satisfactorily fitted to an equivalent circuit consisting of four RC meshes in series.⁴ On the basis of the potential dependence of the resulting circuit elements, these meshes could be straightforwardly ascribed to four substructural elements of the tBLM, namely, the lipoic acid residue, the TEO moiety, the lipid-bilayer moiety, and the aqueous solution bathing the tBLM. These substructural elements of the tBLM were correlated to the RC meshes of the equivalent circuit by a novel approach based on a model of the electrified interface and on the kinetics of ion translocation across potential-energy barriers.

This work describes an investigation of ion transport by the channel-forming protein OmpF porin incorporated in the above mercury-supported tBLM, carried out by electrochemical impedance spectroscopy. An impedance spectroscopy study of OmpF porin in lipid bilayers supported by indium tin oxide (ITO) electrodes was carried out by Gritsch et al.⁶ One goal of the present work was to reconstitute channel-forming proteins into preformed tBLMs without using vesicles in their preparation and proteoliposomes in protein incorporation. This excludes the possibility of adsorption on the tBLM of partially fused vesicles,

* Corresponding author. E-mail: rolando.guidelli@unifi.it.

(1) Guidelli, R.; Aloisi, G.; Becucci, L.; Dolfi, A.; Moncelli, M. R.; Tadini Buoninsegni, F. *J. Electroanal. Chem.* **2001**, *504*, 1–28.

(2) (a) Lang, H.; Duschl, C.; Vogel, H. *Langmuir* **1994**, *10*, 197–210. (b) Steinem, C.; Janshoff, A.; von dem Bruch, K.; Reihs, K.; Goossens, J.; Galla, H.-J. *Bioelectrochem. Bioenerg.* **1998**, *45*, 17–26. (c) Cornell, B. A.; Braach-Maksvytis, V. L. B.; King, L. G.; Osman, P. D. J.; Raguse, B.; Wiczorek, L.; Pace, R. J. *Nature* **1997**, *387*, 580–583. (d) Naumann, R.; Jonczyk, A.; Kopp, R.; van Esch, J.; Ringsdorf, H.; Knoll, W.; Gräber, P. *Angew. Chem., Int. Ed. Engl.* **1995**, *34*, 2056–2058. (e) Bunjes, N.; Schmidt, E. K.; Jonczyk, A.; Rippmann, F.; Beyer, D.; Ringsdorf, H.; Gräber, P.; Knoll, W.; Naumann, R. *Langmuir* **1997**, *13*, 6188–6194. (f) Heyse, S.; Ernst, O. P.; Dienes, Z.; Hofmann, K. P.; Vogel, H. *Biochemistry* **1998**, *37*, 507–522. (g) Schmidt, E. K.; Liebermann, T.; Kreiter, M.; Jonczyk, A.; Naumann, R.; Offenhäusser, A.; Neumann, E.; Kukol, A.; Maelicke, A.; Knoll, W. *Biosens. Bioelectron.* **1998**, *13*, 588–591. (h) Naumann, R.; Schmidt, E. K.; Jonczyk, A.; Fendler, K.; Kadenbach, B.; Liebermann, T.; Offenhäusser, A.; Knoll, W. *Biosens. Bioelectron.* **1999**, *14*, 651–662.

(3) (a) Becucci, L.; Moncelli, M. R.; Guidelli, R. *Langmuir* **2003**, *19*, 3386–3392. (b) Moncelli, M. R.; Becucci, L.; Schiller, S. M. *Bioelectrochemistry*, **2004**, *63*, 161–167.

(4) Becucci, L.; Moncelli, M. R.; Guidelli, R. *J. Am. Chem. Soc.* **2005**, *127*, 13316–13323.

(5) (a) Naumann, R.; Schiller, S. M.; Gieß, F.; Grohe, B.; Hartman, K. B.; Kärcher, I.; Köper, I.; Lübben, J.; Vasilev, K.; Knoll, W. *Langmuir* **2003**, *19*, 5435–5443. (b) Naumann, R.; Walz, D.; Schiller, S. M.; Knoll, W. *J. Electroanal. Chem.* **2003**, *550*–551, 241–247. (c) Schiller, S. M.; Naumann, R.; Lovejoy, K.; Kunz, H.; Knoll, W. *Angew. Chem., Int. Ed. Engl.* **2003**, *42*, 208–211.

(6) Gritsch, S.; Nollert, P.; Jähnig, F.; Sackmann, E. *Langmuir* **1998**, *14*, 3118–3125.

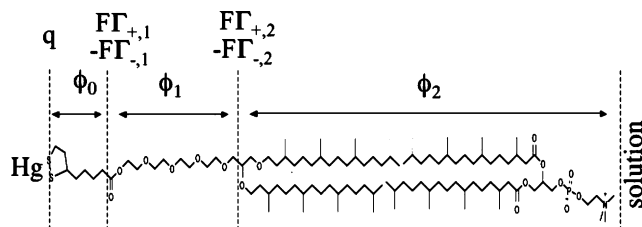


Figure 1. Primary structure of the tBLM, with the various substructural elements and the assumed distribution of charges.

the solution side of which may represent a preferential site for protein incorporation.

Materials and Methods

The water used was obtained from water produced by an inverted osmosis unit, upon distilling it once and then distilling the water thus obtained from alkaline permanganate. Merck Suprapur KCl was baked at 500 °C before use to remove any organic impurities. Diphtanoylphosphatidylcholine (DphyPC) was purchased from Avanti Polar Lipids (Birmingham, AL). The 2,3-di-*O*-phytanyl-*sn*-glycerol-1-tetraethylene-glycol-D,L- α lipoic acid ester lipid (DPTL) was a generous gift of Prof. Wolfgang Knoll and Dr. Renate Naumann from the Max Plank Institute for Polymer Research in Mainz (Germany). An aqueous solution of 1.6 mg/mL OmpF porin in a pH 7.3 buffer containing 20 mM NaH₂PO₄ and 1% octyl-polyoxyethylene (octyl-POE) was a generous gift of Prof. T. Schirmer and Dr. G. L. Orris from Basel University (Switzerland). The other chemicals and solvents were commercially available and used as received.

All measurements were carried out in aqueous 0.1 M KCl. A homemade hanging mercury drop electrode (HMDE), described elsewhere,⁷ was employed. Use was made of a homemade glass capillary with a finely tapered tip, about 1 mm in outer diameter. Capillary and mercury reservoirs were thermostated at 25 ± 0.1 °C by the use of a water-jacketed box to avoid any changes in drop area due to a change in temperature. One glass cell containing the 0.1 M KCl aqueous solution and a small glass vessel containing the ethanol solution of the thiolipid were placed on a movable support inside the box.⁸ The HMDE and the support were moved vertically and horizontally, respectively, by means of two oleodynamic systems that ensured the complete absence of vibrations. AC voltammetry and impedance spectroscopy measurements were carried out with a PGSTAT12 instrument (Echo Chemie) supplied with an FRA2 module for impedance measurements, a SCAN-GEN scan generator, and GPES and FRA software (4.9.005 Beta). Potentials were measured versus a Ag|AgCl 0.1 M, but are referenced to a saturated calomel electrode (SCE).

DphyPC solutions were prepared by diluting a proper amount of stock solution of this phospholipid with pentane. Solutions of 0.2 mg/mL DPTL in ethanol were prepared from a 2 mg/mL solution of DPTL in ethanol. Stock solutions of this thiolipid and the aqueous solution of OmpF were stored at -18 °C. Monolayers of DPTL were self-assembled on the HMDE by keeping the mercury drop immersed in the small vessel containing a 0.2 mg/mL solution of DPTL in ethanol for 20 min. Using the oleodynamic system, the DPTL-coated HMDE was then extracted from the vessel and washed with ethanol to remove the excess of adsorbed thiolipid. Subsequently, the cell, containing a deaerated aqueous solution of 0.1 M KCl, on whose surface a film of DphyPC had been previously spread, was brought below the HMDE, and the drop was kept in a N₂ atmosphere to allow the solvent to evaporate. The drop was then lowered and immersed into the aqueous solution across the phospholipid film; this procedure causes a DphyPC monolayer to self-assemble on top of the DPTL monolayer, forming the tBLM. The applied potential was then repeatedly scanned over a potential range from -0.200 to -1.200 V while the quadrature component of the electrode

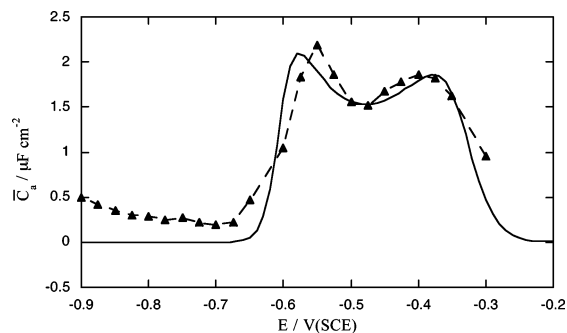


Figure 2. Experimental plot of \bar{C}_a (solid triangles) against E at a tBLM incorporating OmpF porin, in 0.1 M KCl. The solid curve is a fit to the experimental plot calculated from the model for the lipid monolayer moiety using the following parameters: $K_{+,1} = 5 \times 10^{-3}$, $K_{+,2} = 3 \times 10^5 \text{ cm}^3 \text{ mol}^{-1}$; $K_{-,1} = 5 \times 10^{-3}$, $K_{-,2} = 3 \text{ cm}^3 \text{ mol}^{-1}$; $C_0 = 4 \mu\text{F cm}^{-2}$; $C_1 = 7 \mu\text{F cm}^{-2}$; $C_2 = 1 \mu\text{F cm}^{-2}$; $\chi_1 = -0.250 \text{ V}$; $\Gamma_m = 1 \times 10^{-11} \text{ mol cm}^{-2}$; $a' = a'' = 500 \text{ V}^{-1}$; $\Delta' = 0.130 \text{ V}$; and $\Delta'' = 0.165 \text{ V}$. The ordinates refer to the calculated curve. The vertical axis of the experimental plot is arbitrary: this plot was forced to coincide with the calculated curve at the position of the minimum.

admittance, Y'' , was continuously monitored by AC voltammetry at a frequency of 75 Hz; the scanning was stopped when a stable Y'' versus potential curve was attained. Over the potential range from -0.200 to -1.200 V, Y'' assumes values corresponding to a capacity $C = Y''/\omega$, ranging from 0.55 to 0.65 $\mu\text{F cm}^{-2}$, where ω is the angular frequency.

Reconstitution of OmpF in the tBLM was carried out by adding to the cell containing the 0.1 M KCl aqueous solution the stock solution of the protein to obtain a final OmpF concentration of 130 ng/mL. The resulting octyl-POE concentration in the cell was verified to have no effect on the impedance spectrum of an OmpF-free tBLM. After OmpF was added, the solution was stirred for a few minutes while the electrode was kept at an applied potential of -0.2 V. OmpF was added only after it was verified that such a stirring had no effect on the capacity of the tBLM. No appreciable difference was observed between the impedance spectra obtained in unbuffered solutions of 0.1 M KCl and those obtained in solutions buffered at pH 7 with a 10⁻³ M phosphate buffer.

Results

Impedance spectra of tBLMs incorporating OmpF were recorded in 0.1 M KCl over a potential range from -0.3 to -0.95 V and over a frequency range from 1 × 10⁻² to 1 × 10⁵ Hz. The presence of OmpF increases both the in-phase and the quadrature components of the tBLM impedance. In a previous work,⁴ it was shown that the impedance spectra of these tBLMs, both in the absence and in the presence of the ionophore valinomycin, can be satisfactorily fitted to an equivalent circuit consisting of four RC meshes in series; each RC mesh can be ascribed to a substructural element of the tBLM. The same equivalent circuit was adopted in the present work. However, unlike valinomycin, which was incorporated into the supported lipid bilayer from its aqueous solution, OmpF could not be incorporated into the tBLM in a reproducible amount. Consequently, the values of the circuit elements extracted from the fitting vary somewhat from one tBLM to another. Nonetheless, their dependence upon the applied potential is not affected to an appreciable extent by the amount of incorporated OmpF, apart from a scaling factor. Therefore, attention will be focused on the qualitative features of the potential dependence of these circuit elements by plotting this dependence on an arbitrary scale.

Figure 2 shows a plot of the capacity, \bar{C}_a , of one of the RC meshes against the applied potential E . \bar{C}_a exhibits a minimum at -0.48 V and two sharp maxima at -0.55 and -0.40 V. The

(7) Moncelli, M. R.; Becucci, L. *J. Electroanal. Chem.* **1997**, 433, 91–96.

(8) Tadini Buoinsegna, F.; Herrero, R.; Moncelli, M. R. *J. Electroanal. Chem.* **1998**, 452, 33–42.

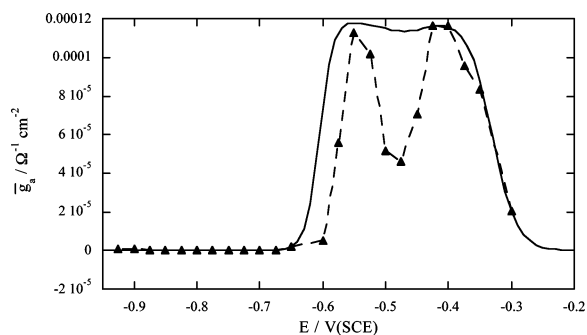


Figure 3. Experimental plot of \bar{g}_a (solid triangles) against E at a tBLM incorporating OmpF porin, in 0.1 M KCl. The solid curve is a fit to the experimental plot calculated from the model for the lipid-bilayer moiety using the same parameters used in Figure 2 and, in addition, $\alpha = 0.5$, $k_{+1} = k_{-1} = 4 \times 10^{16} \text{ cm}^2 \text{ s}^{-1} \text{ mol}^{-1}$, $k_{+2} = 0.1 \text{ s}^{-1}$, and $k_{-2} = 1 \times 10^4 \text{ s}^{-1}$. The ordinates refer to the calculated plot. The vertical axis of the experimental plot is arbitrary: this plot was forced to coincide with the calculated curve at the position of the maximum.

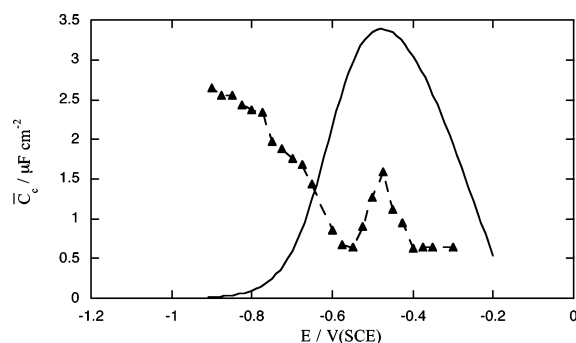


Figure 4. Experimental plot of \bar{C}_c (solid triangles) against E at a tBLM incorporating OmpF porin, in 0.1 M KCl. The solid curve was calculated from the model for the TEO moiety using the same parameters used in Figure 2.

potential dependence of the corresponding conductance, \bar{g}_a , shown in Figure 3, parallels that of the capacity.

The capacity \bar{C}_b and conductance \bar{g}_b of a second RC mesh show a potential dependence that is analogous to those in Figures 2 and 3; more precisely, on the same tBLM, the magnitude of \bar{C}_b is comparable to that of \bar{C}_a , while \bar{g}_b is about 2 orders of magnitude less than \bar{g}_a . The general approach discussed in the following section allows the above two RC meshes to be ascribed to the lipid-bilayer moiety; in particular, mesh *a* is attributed to the section of the lipid bilayer incorporating the vestibular portion of the OmpF channel, and mesh *b* is attributed to the section incorporating the narrow pore.

The capacity \bar{C}_c of the third RC mesh does not vary appreciably on different tBLMs; it is reported in Figure 4 against the applied potential E . It is very low at the more positive potentials, shows a peak at about -0.48 V , and then increases gradually toward more negative potentials. As discussed in the following section, the peak agrees qualitatively with that predicted by the model for the TEO moiety, while the rising portion of the plot at more negative potentials is reminiscent of the behavior of the lipoic acid residue. Therefore, mesh *c* can be tentatively interpreted by assuming that the time constants of the lipoic acid residue and of the TEO moiety are too close to allow the fitting of the impedance spectra to resolve the corresponding RC meshes. On all tBLMs tested, the capacity C_d of the fourth RC mesh in 0.1 M KCl is approximately equal to 25 nF cm^{-2} , and the corresponding conductance, g_d , is approximately equal to $0.3 \text{ } \Omega^{-1} \text{ cm}^{-2}$; these quantities are identical to those measured on

a tBLM in the absence of OmpF. Moreover, C_d and g_d are proportional to the KCl concentration. The fourth mesh must, therefore, be ascribed to the aqueous solution adjacent to the tBLM⁴ and will not be considered further.

Discussion

The symbols of the capacities and conductances of the first three RC meshes are overbarred, to distinguish them from the “intrinsic” conductances and capacities of the substructural elements composing the tBLM in the absence of OmpF. In fact, the potential dependence of the circuit elements of the first three meshes is related to the gradual change in the amount and nature of the ions being accommodated in the TEO hydrophilic spacer with varying the applied potential. To interpret the behavior of the three meshes, with particular regard to the potential dependence of their circuit elements, use will be made of a model of the electrified interphase and of its kinetic treatment under AC conditions.

Even though K^+ and Cl^- ions are distributed in space across the tBLM, albeit nonhomogeneously, the ideal circuit elements used for the fitting represent ideal lumped-constant properties. To find a correspondence between these circuit elements and the tBLM structure, the charges within the tBLM will be assumed to be located as follows (see Figure 1): a free electronic charge density, q , on the surface of the mercury electrode, two charge densities, FT_{+1} and $-FT_{-1}$, at the boundary between the lipoic acid residue and the TEO moiety, and two charge densities, FT_{+2} and $-FT_{-2}$, at the boundary between the TEO moiety and the lipid bilayer. Here, Γ_{+1} , Γ_{+2} and Γ_{-1} , Γ_{-2} are surface concentrations of K^+ and Cl^- ions, respectively. This charge distribution leads to the following expression for the extrathermodynamic potential difference ϕ_t across the whole electrified interphase:⁴

$$\phi_t = \frac{q}{C_0} + \left[\frac{q + F(\Gamma_{+1} - \Gamma_{-1})}{C_1} + \chi_1 \right] + \frac{q + F(\Gamma_{+1} - \Gamma_{-1} + \Gamma_{+2} - \Gamma_{-2})}{C_2} \equiv \phi_0 + \phi_1 + \phi_2 \quad (1)$$

Here, C_0 , C_1 , and C_2 are the “intrinsic” capacities of the lipoic acid residue, the TEO moiety, and the lipid bilayer, respectively, as measured in the absence of OmpF, while ϕ_0 , ϕ_1 , and ϕ_2 are the potential differences across these dielectric slabs. ϕ_1 includes the dipole potential, χ_1 , of the TEO moiety, which was estimated at about -0.250 V , negative toward the metal, on the basis of independent measurements.^{3b} Several pieces of experimental evidence indicate that the extrathermodynamic absolute potential difference ϕ_t across the whole mercury|aqueous solution interphase is more positive than the potential E measured versus an SCE by about 0.250 V .^{3a} Therefore, ϕ_t can be directly related to the applied potential E .

The fitting program regards the circuit elements of the three RC meshes as frequency-independent and independent of each other along each impedance spectrum at constant E , albeit allowing for their variation with a change in E , because of their dependence upon the various surface concentrations. To relate the potential dependence of the circuit elements in Figures 2 and 3 to the equilibrium and kinetic properties of the above model of the electrified interphase, a general approximate approach, outlined in the Supporting Information (SI) file available on the Web, is adopted. The numbers of the equations reported in the SI file are preceded by the letter A, which stands for Appendix.

The main assumptions made in this approach are as follows. The small perturbation, Δj , in the current that flows to and from any of the two dielectric slabs representing the TEO moiety and the lipid bilayer, and which charges and discharges the two boundaries of the corresponding slab, is equated to sum of the time derivatives of the perturbations, $F\Delta\Gamma_+$ and $-F\Delta\Gamma_-$, in the charges of K^+ and Cl^- ions on the metal side of the slab (eq A1). In view of the small AC perturbation, ΔE , in the applied potential, Δj is also regarded as a linear function of $\Delta\Gamma_+$, $\Delta\Gamma_-$, and ΔE (eq A2). The current, j_{+2} , flowing along the lipid-bilayer moiety and requiring K^+ ions to surmount the corresponding potential-energy barrier, is expressed by a Butler–Volmer-like equation (eq A8), where \bar{k}_{+2} and \bar{k}_{-2} are the corresponding forward and backward rate constants for $\phi_2 = 0$, respectively. Under equilibrium conditions, namely, for $j_{+2} = 0$, this equation reduces to a Langmuir isotherm, with a potential-independent adsorption equilibrium constant $K_{+2} = \bar{k}_{+2}/\bar{k}_{-2}$ (eq A9). An analogous equation is written for the current, j_{-2} , requiring Cl^- ions to surmount the potential-energy barrier due to the lipid-bilayer moiety (eq A10), where \bar{k}_{-2} and \bar{k}_{+2} are the corresponding forward and backward rate constants for $\phi_2 = 0$, respectively, and $K_{-2} = \bar{k}_{-2}/\bar{k}_{+2}$ is the corresponding adsorption equilibrium constant (eq A11). Butler–Volmer-like equations are also used to express the currents, j_{+1} and j_{-1} , due to the translocation of K^+ and Cl^- ions across the TEO moiety (eqs A15 and A17), where \bar{k}_{+1} , \bar{k}_{-1} and \bar{k}_{-1} , \bar{k}_{+1} are the corresponding forward and backward rate constants for $\phi_1 = 0$, while $K_{+1} = \bar{k}_{+1}/\bar{k}_{-1}$ and $K_{-1} = \bar{k}_{-1}/\bar{k}_{+1}$ are the corresponding adsorption equilibrium constants (eqs A16 and A18).

To predict the position of the minimum in the \bar{C}_a versus E curve in Figure 2 on the basis of the model, the same parameters obtained in ref 4 for the tBLM in the absence of incorporated ion carriers were employed, namely, the intrinsic capacities $C_0 = 4 \mu F cm^{-2}$, $C_1 = 7 \mu F cm^{-2}$, and $C_2 = 1 \mu F cm^{-2}$ and the dipole potential $\chi_1 = -0.250$ V. Moreover, the maximum surface concentration Γ_m attained by $(\Gamma_{+1} + \Gamma_{-1})$ and by $(\Gamma_{+2} + \Gamma_{-2})$, as well as the equilibrium constants for the translocation of K^+ ions across the TEO moiety and across the lipid bilayer, were set equal to the values, $\Gamma_m = 1 \times 10^{-11} mol cm^{-2}$, $K_{+1} = 5 \times 10^{-3}$, and $K_{+2} = 3 \times 10^5 cm^3 mol^{-1}$, which were found to provide the best fit to the impedance spectra of a tBLM in contact with aqueous 0.1 M KCl and incorporating valinomycin as an ion carrier.⁴ In fact, the equilibrium distribution of these ions on the two sides of the lipid bilayer should be independent of the nature of the ion carrier. The equilibrium constant, K_{-1} , for the translocation of Cl^- ions across the TEO moiety is expected to be close to that for K^+ ions; consequently, K_{-1} was set equal to 5×10^{-3} .

Incidentally, the low Γ_m value used for the fitting, which corresponds to a charge density of about $1 \mu C cm^{-2}$, is an adjustable parameter that bears no direct relation to the maximum charge that can be accommodated in the hydrophilic spacer. The ions are clearly distributed throughout the whole hydrophilic spacer; consequently, the microscopic properties of the latter may also be distributed. In this case, a single ideal RC mesh for the TEO moiety may be inadequate to describe its electrical response. An approximate approach may consist of simulating the distribution of ions throughout the whole TEO moiety by a series of an arbitrary number, m , of identical ideal RC meshes of capacity \bar{C}_m ; the overall capacity of this series is equal to \bar{C}_m/m . Consequently, the $\mathcal{Z}(\Delta\Gamma_{\pm i})/\mathcal{Z}(\Delta E)$ ratios in eq A7 are also divided by m , and the same is true for the actual maximum surface concentration. As a matter of fact, these m RC meshes cannot be exactly identical in the presence of ion transport, and

their properties are expected to vary gradually in passing from one end of the TEO to the other end. In the present approach, these differences in properties are exclusively located at the two ends of the TEO, but with an arbitrary low value of Γ_m .

Upon using the above parameters, extracted from the impedance spectra of a tBLM incorporating valinomycin, we are left with only one adjustable parameter, namely, the equilibrium constant K_{-2} for the Cl^- translocation across the lipid bilayer. The potential, -0.48 V, at the \bar{C}_a versus E minimum is predicted for a K_{-2} value of $3 cm^3 mol^{-1}$, which is 5 orders of magnitude less than K_{+2} . Note that adjusting the K_{-2} parameter so as to account for the \bar{C}_a versus E minimum amounts to ascribing the \bar{C}_a and \bar{g}_a circuit elements to the lipid-bilayer moiety. At this minimum, the surface concentrations Γ_{+2} and Γ_{-2} are equal so as to compensate their opposite charges, as expected. This implies that eqs A9 and A11 are also equal at the minimum. From this equality, and from eqs A13 and A14, it follows that the calculated potential, $+150$ mV, across the lipid-bilayer moiety (i.e., the transmembrane potential) at the minimum, $\phi_{2,min}$, is given by the expression

$$\phi_{2,min} = +150 \text{ mV} = \frac{RT}{2F} \ln \frac{K_{+2}}{K_{-2}} = \frac{\mu_{-2}^0 - \mu_{+2}^0}{2F} \quad (2)$$

Here, μ_{-2}^0 and μ_{+2}^0 are the formal chemical potentials of the Cl^- and K^+ ions, respectively, on the solution side of the TEO moiety. In writing eq 2, the reasonable assumption was made that the formal chemical potentials of the Cl^- and K^+ ions in the aqueous solution are equal.

The $\phi_{2,min}$ quantity is practically equivalent to the zero-current membrane potential V_m of a bilayer lipid membrane (BLM), in that it refers to a situation in which the local concentration of the anion is equal to that of the cation on each of the two sides of the lipid bilayer, and the current across the lipid bilayer is practically equal to zero. The cation selectivity of OmpF is well documented.⁹ In particular, the P_K/P_{Cl} permeability ratio was estimated at 15.5, which corresponds to a V_m value of $+46$ mV, under 0.01 M KCl/0.1 M KCl conditions.^{9c} Even though the exact “volume” concentration of KCl on the solution side of the TEO moiety at the \bar{C}_a minimum is unknown, it is almost certainly less than its value in the solution bathing the tBLM. However, the $+150$ mV value for the transmembrane potential $\phi_{2,min}$ seems too high to be exclusively ascribed to a P_K/P_{Cl} permeability ratio across the lipid-bilayer moiety of the tBLM strongly in favor of K^+ ions. The appreciable difference between the present $\phi_{2,min}$ value and that derived from the literature values of the P_K/P_{Cl} permeability ratio can quite probably be ascribed to specific attractive interactions of K^+ ions with the etheric oxygen atoms of the TEO moiety not shared by Cl^- ions. This implies that the difference, $\mu_{-2}^0 - \mu_{+2}^0$, in the formal chemical potentials of Cl^- and K^+ ions, which accounts for a difference in the specific interactions of these two ions with the TEO moiety, is expected to be positive. In view of eq 2, this makes a positive contribution to $\phi_{2,min}$, which is added to the contribution from the positive P_K/P_{Cl} permeability ratio.

A positive $\mu_{-2}^0 - \mu_{+2}^0$ value may also possibly justify the narrow range of potentials over which the presence of OmpF increases the \bar{C}_a , \bar{g}_a and \bar{C}_b , \bar{g}_b values of the tBLM with respect to those in its absence. It has been shown that OmpF, once

(9) (a) Benz, R.; Janko, K.; Läuger, P. *Biochim. Biophys. Acta* **1979**, *551*, 238–247. (b) Saint, N.; Lou, K.-L.; Widmer, C.; Luckey, M.; Schirmer, T.; Rosenbusch, J. P. *J. Biol. Chem.* **1996**, *271*, 20676–20680. (c) Danelon, C.; Suenaga, A.; Winterhalter, M.; Yamato, I. *Biophys. Chem.* **2003**, *104*, 591–603. (d) Alcaraz, A.; Nestorovich, E. M.; Aguilera-Arzo, M.; Aguilera V. M.; Bezrukov, S. M. *Biophys. J.* **2004**, *87*, 943–957.

reconstituted in BLMs, undergoes closure when transmembrane potentials of ± 130 to ± 200 mV are applied.¹⁰ In the present case, we may express the probability of the OmpF channels passing from the open to the closed state on both sides of the capacity minimum by a double-sided Boltzmann equation:¹¹

$$\frac{1}{1 + \exp[-a'(\phi_2 - \Delta')]} \times \frac{1}{1 + \exp[a''(\phi_2 - \Delta'')]} \quad (3)$$

This is just the product of two one-sided Boltzmann equations, which express the probability p of one channel being in the open state. The first factor accounts for the rising branch of the \bar{C}_a versus E plot on the negative side of the minimum; the second accounts for the descending branch on the positive side. A relatively satisfactory fit is obtained for $a' = 500 \text{ V}^{-1}$, $\Delta' = 0.130 \text{ V}$, $a'' = 500 \text{ V}^{-1}$, and $\Delta'' = 0.165 \text{ V}$, as shown by the solid curve in Figure 2. The Δ' and Δ'' values indicate that a 0.5 value for the probability of the OmpF channels being open is attained at a transmembrane potential $\phi'_2 = +130$ mV on the negative side of the \bar{C}_1 minimum and at $\phi''_2 = +165$ mV on the positive side. While the ϕ''_2 value is in fairly good agreement with that reported on BLMs,⁹ the ϕ'_2 value is shifted in the positive direction by about 300 mV. This denotes a notable difficulty encountered by OmpF channels incorporated in the tBLM to open when proceeding toward more positive potentials with respect to BLMs.

This difference in behavior can possibly be explained by considering the general expression for the one-sided Boltzmann equation:¹²

$$\frac{1}{1 + \left\{ \frac{q_g}{kT} \left[(\phi_c - \phi_o) + \frac{\mu_c^0 - \mu_o^0}{q_g} \right] \right\}} \quad (4)$$

Here, q_g is the "gating" charge, ϕ_c and ϕ_o are the electrostatic potentials at the position occupied by the gating charge in the closed and open states, respectively, and μ_c^0 and μ_o^0 are the formal chemical potentials of the channel in the closed and open states, respectively. In practice, $\mu_c^0 - \mu_o^0$ measures the change in the conformational energy of the channel in passing from the open to the closed state. The opening of a voltage-gated channel in the direction of positive potentials requires a movement of a positive gating charge toward the solution side of the lipid-bilayer moiety and/or a movement of a negative gating charge toward the metal side. If q_g is negative and moves across the whole "dielectric" thickness of the OmpF channel to open it, then $\phi_c - \phi_o$ is practically equal to the opposite of the transmembrane potential ϕ_2 , which measures the potential on the metal side of the lipid-bilayer moiety with respect to that on the solution side. This assumption is reasonable since the OmpF channel consists of both an extracellular and a periplasmic vestibule, with a narrow pore interposed between the two;¹³ the pore includes the narrowest part of it, called the "constriction zone". In this respect, the dielectric thickness can be roughly identified with the thickness of the narrow pore. During the

channel opening, the negative gating charge can, therefore, be assumed to pass from the aqueous medium to a medium of lower hydrophilicity, where, in addition, the lower concentration of ions decreases the screening of the charge. This implies an increase in the chemical potential of the gating charge, with a resulting negative contribution to $\mu_c^0 - \mu_o^0$ with respect to its value in a BLM. In the present case, the expression between the braces in eq 4 takes the form $\{-|q_g|[\phi_2 - (\mu_c^0 - \mu_o^0)/q_g]/kT\}$, from which it is apparent that the positive contribution to the $(\mu_c^0 - \mu_o^0)/q_g$ ratio requires an increase in the positive value of ϕ_2 to attain the same probability of the channel being open that is found in a BLM. In other words, the work to be spent by a negative gating charge to pass from the aqueous medium to a less hydrophilic medium requires a more positive transmembrane potential ϕ_2 . Clearly, an opposite conclusion would be reached if the channel opening were caused by the movement of a positive gating charge toward the solution side of the lipid bilayer, namely, from the TEO moiety to the aqueous solution. Consequently, the notable positive shift in the ϕ_2 value at which the channel opens toward more positive potentials, when passing from a BLM to the tBLM, suggests that the gating charge is negative and moves toward the metal side of the lipid bilayer. The magnitude of this charge can be roughly estimated by noting that the experimental value of a' in eq 3, 500 V^{-1} , corresponds to the quantity $|q_g|/kT$ in eq 4. This yields a q_g value approximately equal to $-12 e$. It is possible that this value overestimates the magnitude of the gating charge, but a relatively high gating charge is not unreasonable when we consider that the net charge of the OmpF trimer at pH 7 is $-30 e$.¹⁴

The potential dependence of the conductance \bar{g}_a can be predicted qualitatively by the model, using the same parameters adopted for the capacity \bar{C}_a and four additional adjustable parameters expressing the backward rate constants for the translocation of K^+ and Cl^- ions across the lipid bilayer and the TEO moiety, as shown in Figure 3. Incidentally, the $\bar{k}_{+,1}$ and $\bar{k}_{+,2}$ values are identical to those providing the best fit to the conductance of tBLMs incorporating valinomycin.⁴ The calculated minimum at -0.48 V is much shallower than the experimental one.

The capacity \bar{C}_b and conductance \bar{g}_b of the second RC mesh exhibit a potential dependence very close to those of \bar{C}_a and \bar{g}_a , even though \bar{g}_b is 2 orders of magnitude lower than \bar{g}_a . This behavior can be tentatively explained by ascribing mesh a to the vestibular portion of the OmpF channel, and mesh b to the portion of the narrow pore.

The potential dependence of \bar{C}_c in Figure 4 is difficult to interpret. The low value of this capacitance and its gradual increase toward more negative potentials is reminiscent of the capacity of the RC mesh ascribed to the lipoic acid residue in a tBLM not incorporating ion carriers or channels (see Figure 6a in ref 4). However, the capacity peak at about -0.50 V in Figure 4 is not present in the C versus E plot ascribed to the lipoic acid residue, while it is predicted by the present model for the TEO moiety in the presence of incorporated OmpF, upon using the same parameters seen in Figure 2 (see the solid curve in Figure 4). The \bar{C}_c versus E plot in Figure 4 can be tentatively interpreted by assuming that the time constants of the lipoic acid residue and of the TEO moiety are close, such that the fitting of the impedance spectra to the equivalent circuit adopted herein cannot resolve the corresponding RC meshes.

In conclusion, the investigation of a biomimetic membrane consisting of a lipid bilayer tethered to mercury via a hydrophilic

(10) (a) Schindler, H.; Rosenbusch, J. P. *Proc. Natl. Acad. Sci. U.S.A.* **1978**, *75*, 3751–3755. (b) Engel, A.; Massalski, A.; Schindler, H.; Dorset, D. L.; Rosenbusch, J. P. *Nature* **1985**, *317*, 643–645.

(11) De Felice, L. *J. Electrical Properties of Cells*; Plenum: New York, 1997; p.136.

(12) Hille, B. *Ion Channels of Excitable Membranes*; Sinauer Associates: Sunderland, MA, 2001; p 57.

(13) (a) Weiss, M.; Schulz, G. *J. Mol. Biol.* **1992**, *227*, 493–509. (b) Cowan, S.; Schirmer, T.; Rummel, G.; Steiert, M.; Ghosh, R.; Paupit, R. et al. *Nature* **1992**, *358*, 727–733. (c) Schulz, G. *Curr. Opin. Struct. Biol.* **1996**, *6*, 485–490. (d) Schirmer, T. *J. Struct. Biol.* **1998**, *121*, 101–109.

spacer by electrochemical impedance spectroscopy yields information on the structure of the membrane and on the effect of the incorporation of ion channels in the bilayer, provided the analysis covers a sufficiently broad potential range. Fitting the impedance spectra to a series of RC meshes allows these meshes to be ascribed to different substructural elements of the tBLM on the basis of their dependence upon the applied potential. This dependence, which is due to the gradual filling of the hydrophilic portion of the tBLM by ions moving along the ion channel as the applied potential is varied, can be interpreted on the basis of a general approximate approach. Application of the present technique to the investigation of the channel-forming peptides gramicidin and melittin is in progress.

Acknowledgment. The authors are grateful to W. Knoll and R. Naumann (Max Planck Institute for Polymer Science, Mainz,

Germany) for providing them with the DPTL thiolipid and T. Schirmer and G. L. Orris (Biocentrum, Basel University, Switzerland) for providing them with OmpF porin. Thanks are due to the Ministry of Education, University and Research (MUIR) of Italy for financial support through PRIN projects and to Ente Cassa di Risparmio di Firenze for financial support through the PROMELAB project.

Supporting Information Available: A general approximate approach, which applies the concepts of impedance spectroscopy to a model of the electrified interphase and to the kinetics of potassium and chloride ion transport across the tBLM. This material is available free of charge via the Internet at <http://pubs.acs.org>

LA0520839